

The host galaxies of AGN in the Sloan Digital Sky Survey

Timothy M. Heckman^{a,*}, Guinevere Kauffmann^b

^a Center for Astrophysical Sciences, Department of Physics and Astronomy, The Johns Hopkins University, Baltimore, MD 21218, USA

^b Max-Planck-Institute for Astrophysics, D-85748 Garching, Germany

Available online 26 July 2006

Abstract

We summarize recent investigations into the relation between the evolution of black holes and galaxies based on optical spectra from the Sloan Digital Sky Survey. The galaxy population exhibits a remarkably simple bimodal behavior in age and structure as a function of mass. Strong emission-line AGN (Seyferts) inhabit those unusual galaxies that are both relatively massive and dense, yet have a significant young stellar population. A volume average over the SDSS sample, shows that the population of black holes with masses less than $\sim 10^{7.5} M_{\odot}$ is growing rapidly at the current epoch. The population of more massive black holes (“dead QSOs”) is quiescent, with weak activity traced by low-power radio sources. For the population of bulge-dominated galaxies as-a-whole, the volume-averaged ratio of the rates of star formation to black hole accretion in the present universe is of-order a thousand (similar to the ratio of stellar and black hole mass in galaxy bulges today). The processes that established this ratio in the fossil record are still at work today, albeit preferentially in less massive black holes and bulges.

© 2006 Elsevier B.V. All rights reserved.

Contents

1. Introduction	678
2. Methodology	678
2.1. The Sloan Digital Sky Survey	678
2.2. Two AGN samples	678
2.3. Derived galaxy parameters	678
2.4. Derived AGN properties	679
3. Results	679
3.1. The SDSS galaxy landscape	679
3.2. Hosts of emission-line AGN	679
3.3. Hosts of radio-loud AGN	680
4. Black hole growth	680
4.1. Which black holes are growing?	680
4.2. The co-evolution of black holes and bulges	682
5. Summary	683
Acknowledgements	683
References	683

* Corresponding author.

E-mail address: heckman@pha.jhu.edu (T.M. Heckman).

1. Introduction

Over the past few years there have been remarkable developments in our understanding of active galactic nuclei (AGN) and their role in galaxy formation and evolution. There is now compelling evidence (e.g. Genzel et al., 2000) for the existence of the supermassive black holes that were long hypothesized as the power-source for active galactic nuclei (Salpeter, 1964). The local mass density in these black holes is sufficient to have powered the total emission of the AGN population over cosmic time if the accreting material is assumed to radiate with an efficiency near the upper end of the plausible range (Yu and Tremaine, 2002; Marconi et al., 2004). The tight correlation between the mass of the black hole and the velocity dispersion and mass of the galactic bulge within which it resides (Ferrarese and Merritt, 2000; Marconi and Hunt, 2003) is compelling evidence for a close connection between the formation of the black hole and that of its host galaxy (e.g. Kauffmann and Haehnelt, 2000; Granato et al., 2001).

Finally, deep X-ray surveys have recently established that the AGN population exhibits the so-called “cosmic down-sizing”: the space density of AGN with low X-ray luminosities peaks at *lower redshift* than that of AGN with high X-ray luminosities (e.g. Ueda et al., 2003; Hasinger et al., 2005). These results indicate that a substantial amount of the total black hole growth has occurred more recently than would have been deduced based on optical surveys of powerful quasars (Boyle et al., 2000; Fan et al., 2001).

The co-evolution of galaxies and black holes can be directly investigated through deep surveys spanning a broad range in redshift. In the present paper, however, we take a complementary approach and use the Sloan Digital Sky Survey (SDSS) to examine the relationship between galaxies and their supermassive black holes in the present-day Universe. This paper represents a summary of results presented in Kauffmann et al. (2003a – hereafter K03), Heckman et al. (2004 – hereafter H04), Brinchmann et al. (2004 – hereafter B04), and Best et al. (2005 – hereafter B05).

2. Methodology

2.1. The Sloan Digital Sky Survey

The data analyzed in this paper are drawn from the Sloan Digital Sky Survey (York et al., 2000; Stoughton et al., 2002). The SDSS is using a dedicated 2.5-meter wide-field telescope at the Apache Point Observatory to conduct an imaging and spectroscopic survey of about a quarter of the sky. The imaging is conducted in the u , g , r , i , and z bands (Fukugita et al., 1996; Smith et al., 2002) using a drift scan camera (Gunn et al., 1998). The images are calibrated photometrically (Hogg et al., 2001) and astrometrically (Pier et al., 2003) and are used to select galaxies

(Strauss et al., 2002). These are observed with a pair of multi-fiber spectrographs built by Alan Uomoto and his team, with fiber assignment based on an efficient tiling algorithm (Blanton et al., 2003). The data are all spectrophotometrically calibrated using observations of **subdwarf F stars** in each 3° field (Tremonti et al., in preparation).

Our methodology is described in detail in K03. We have written a special purpose code that fits each SDSS galaxy spectrum with a stellar population model (Bruzual and Charlot, 2003) and then subtracts this model to leave a pure emission-line spectrum. The emission-lines are then subtracted from the original spectrum to produce an emission-line-free spectrum to characterize the stellar population.

2.2. Two AGN samples

Starting with the SDSS “main” galaxy sample, we have defined two independent samples of AGN: an optical emission-line sample and a radio-loud sample. The SDSS main galaxy sample explicitly excludes objects in which starlight does not dominate the optical spectrum (so we are missing QSOs and powerful Type 1 Seyfert nuclei). Moreover, the SDSS main galaxy sample has a median redshift of ~ 0.1 , and the surveyed volume is too small to contain many highly powerful AGN. This limitation should be kept in mind in what follows.

Following Baldwin et al. (1981) and Veilleux and Osterbrock (1987), we have first identified AGN based on the flux ratios of two pairs of the strongest narrow emission-lines in their optical spectra: $[\text{OIII}]\lambda 5007/\text{H}\beta$ vs. $[\text{NII}]\lambda 6584/\text{H}\alpha$. These are either LINERs, Type 2 Seyferts, or AGN/star-forming composite objects. See K03 and H04 for details.

Secondly, we have used a combination of the FIRST (Becker et al., 1995) and NVSS (Condon et al., 1998) VLA 20 cm radio continuum surveys to identify the radio-emitting galaxies in the SDSS main galaxy sample. We have then used the optical properties of the galaxies (see below) to remove the minority population of galaxies in which the radio emission is tracing star formation rather than an AGN. Almost none of the radio-loud AGN are the powerful Fanaroff–Riley Class II sources. See B05 for details.

2.3. Derived galaxy parameters

Following Kauffmann et al. (2003b), we have used two age-sensitive spectral features to characterize the stellar population: the 4000 Å break $D_n(4000)$ and the $\text{H}\delta$ absorption-line ($\text{H}\delta_A$). These indices are compared with a large grid of a model galaxy spectra to determine the near-IR (SDSS z -band) stellar mass-to-light ratio. A comparison of the model and observed spectral energy distributions yields a measure of the attenuation of the z -band luminosity by dust. These parameters are then used to determine the stellar mass (M_*) from the **z -band Petrosian magnitude**.

Star formation rates are normally derived for the region sampled by the spectroscopic fiber from the extinction-corrected luminosities of the most prominent emission-lines. These lines cannot be used for galaxies with AGN, and star formation is instead estimated from $D_n(4000)$, based on the strong correlation between $D_n(4000)$ and specific star formation rate SFR/M_* found for galaxies without AGN (see B04).

2.4. Derived AGN properties

For the optical emission-line sample of AGN, we use the luminosity of the [OIII] λ 5007 emission-line as a tracer of AGN activity. This is usually the strongest emission-line in the optical spectra of Type 2 AGN, and it is significantly less contaminated than the others by contributions from star-forming regions (B04; K03; H04). This is important, because the relatively large projected aperture of the SDSS spectra means that such contamination is inevitable.

In H04 we used the large sample of Type 1 AGN in the SDSS (Zakamska et al., 2003; K03) to derive the mean ratio of the [OIII] to the optical continuum luminosity. We then adopted the mean bolometric correction to the optical luminosity derived by Marconi et al. (2004) for QSOs. We verified that the resulting mean bolometric correction factor for the [OIII] luminosity is consistent with values derived for individual Type 1 Seyfert nuclei and QSOs having the appropriate data. We then applied this correction factor to the [OIII] luminosities of Type 2 AGN, assuming that the unified model is correct.

We then used the observed correlation between black hole mass M_{BH} and bulge velocity dispersion σ_* (Tremaine et al., 2002) to derive a black hole mass for all AGN hosts and all SDSS galaxies with substantial bulges (stellar surface mass densities $\mu_* > 3 \times 10^8 M_\odot \text{ kpc}^{-2}$ and $\sigma_* > 70 \text{ km/s}$). Using the AGN bolometric luminosity, we calculated a mass accretion rate, assuming a radiative efficiency of 10%.

3. Results

3.1. The SDSS galaxy landscape

Before describing the properties of the host galaxies of AGN, it is useful to briefly summarize the overall “landscape” of galaxies in the SDSS. As shown in Kauffmann et al. (2003c) and B04, the SDSS galaxy population is strongly bimodal. There are several characteristic scales at which the galaxy population rather abruptly transitions from young (significant on-going star formation) to old (no significant on-going star formation).

Below a stellar mass of $M_* \sim 3 \times 10^{10} M_\odot$, galaxies are young and above this mass they are old. Below a stellar surface mass density of $\mu_* \sim 3 \times 10^8 M_\odot \text{ kpc}^{-2}$, galaxies are young and above this density they are old. Below a Concentration Index of $C \sim 2.6$, galaxies are young and above this they are old. These parameters essentially correspond to a transition from low mass, low density, low con-

centration disk-dominated galaxies to high mass, high density, high concentration bulge-dominated galaxies. Given the close connection between supermassive black holes and the bulge component we would expect that the AGN phenomenon would be confined to the latter population.

3.2. Hosts of emission-line AGN

Fig. 1 summarizes many of the most salient properties of the hosts of emission-line AGN. The top panels show the distribution of stellar mass in all galaxies (not just AGN) partitioned as a function of M_* (right panels) and μ_* (left panels) plotted vs. the age-sensitive index $D_n(4000)$. These panels underscore the bimodal galaxy population described above. In the middle panels, we plot where the [OIII] emission from AGN originates, volume-averaged over the SDSS. These plots then show that most present-day accretion onto black holes is taking place in galaxies with young stellar ages ($D_n(4000) < 1.6$), intermediate to high stellar masses (10^{10} –few $\times 10^{11} M_\odot$), and high surface mass densities (3×10^8 – $3 \times 10^9 M_\odot \text{ kpc}^{-2}$). It is quite remarkable, that the [OIII] emission from AGN peaks just above the transition values of M_* , μ_* , and C (H04) where the galaxy population switches abruptly from young, star-forming and disk-dominated to old, quiescent and bulge-dominated.

In K03 we showed that the stellar population is systematically younger in more powerful AGN. Considering just the powerful AGN (those with extinction-corrected [OIII] luminosities greater than $10^7 L_\odot$), we showed that the typical host galaxy violates the general rules for the SDSS galaxy population. It is a massive, dense, early-type (bulge-dominated) galaxy but has the significant on-going star formation characteristic of the low mass, low density late-type (disk-dominated) galaxies. This is quite evident in the bottom panels of Fig. 1, which shows that the fraction of massive, dense galaxies with young stellar populations that host powerful AGN reaches a value of over 30%.

In K03 we used the broad range in redshift spanned by the SDSS AGN hosts (and the corresponding range in the physical size of the region encompassed by the SDSS spectroscopic fiber) to show that this young stellar population is extended over galactic scales ($\sim 10 \text{ kpc}$). We also showed (by means of stacking the spectra of a large sample of Type 1 Seyferts and QSOs matched in [OIII] luminosity to the most powerful Type 2 AGN) that the stellar populations in the Type 1 and Type 2 AGN are indistinguishable (in accord with the unified model).

As discussed in Kauffmann et al. (2003b), the combination of the $D_n(4000)$ and $H\delta_A$ age-sensitive indices allows us to identify galaxies which have had “bursty” star formation histories over the past Gyr. In K03, we showed that the fraction of AGN hosts with such histories is about three times larger than the fraction of similarly massive normal galaxies. This is an intriguing hint that the growth of black holes may be facilitated by large-scale events that

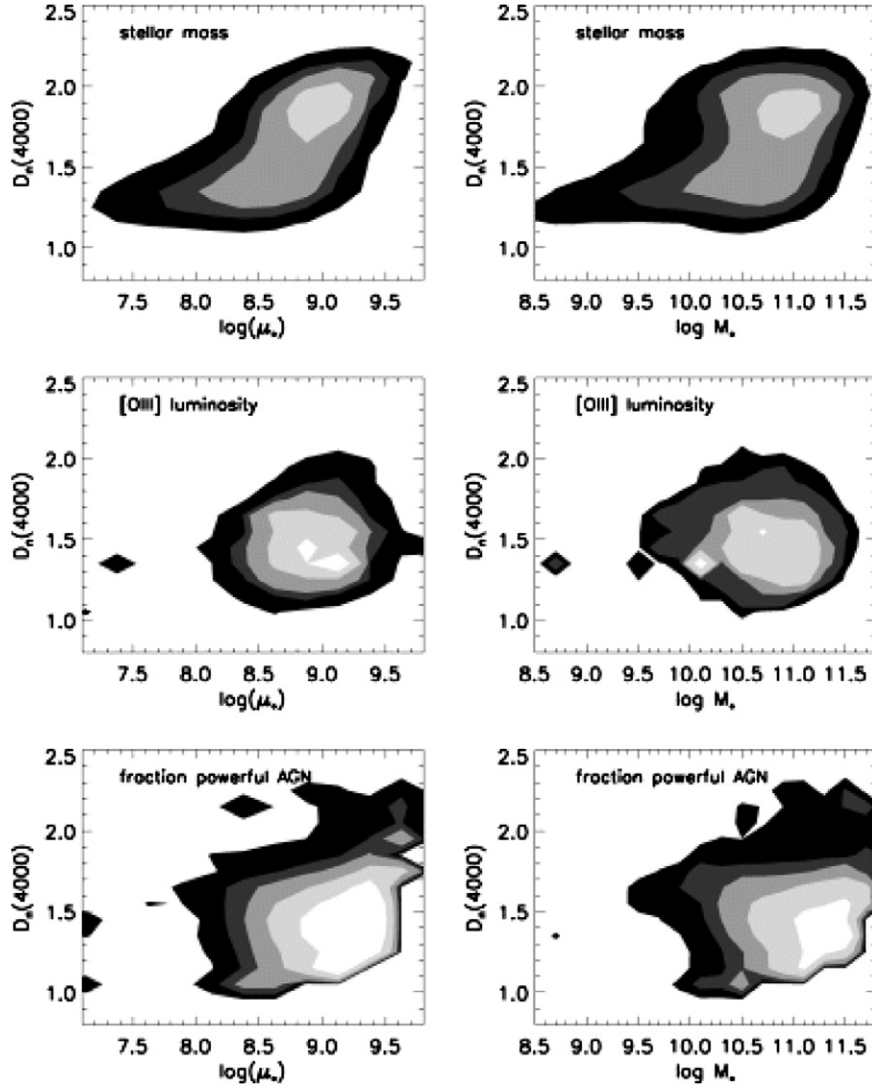


Fig. 1. Top: the distribution of the total stellar mass in the full SDSS galaxy sample in the plane $D_n(4000)$ vs. surface mass density (left) and stellar mass (right). Middle: the distribution of the total AGN [OIII] luminosity. Bottom: the fraction of galaxies that host AGN with $L_{\text{[OIII]}} > 10^7 L_{\odot}$. The contours represent fractions of 0.008, 0.017, 0.035, 0.07, 0.15, and 0.30. See K03 for details.

lead to a significant temporary enhancement in the star formation rate. We hasten to add however, that most of the powerful AGN in the SDSS sample appear to be structurally normal early-type galaxies. Thus, these events would only rarely be major galaxy mergers (see K03).

3.3. Hosts of radio-loud AGN

As shown in B05, the properties of the SDSS radio galaxies are almost disjoint from those of the hosts of the emission-line AGN. One way of seeing this is shown in Fig. 2 which plots the fraction of galaxies that are radio loud as a function of the stellar mass of the host galaxy. The probability at fixed radio power rises very steeply with mass (approximately as $M_*^{2.5}$). This contrasts strongly with what is seen for the emission-line AGN (Fig. 2).

Radio galaxies are therefore preferentially drawn from the most massive portion of the galaxy population. These

large masses, together with their typical structural parameters (average $C \sim 3.2$ and $\mu \sim 10^9 M_{\odot} \text{ kpc}^{-2}$) quantify the long-known result that radio galaxies are generically giant ellipticals. They also differ significantly from the emission-line AGN in their stellar populations: the radio galaxies almost uniformly have the same predominantly old stellar population seen in normal giant ellipticals (B05).

Together, these results strongly suggest that the mode of fueling of low power (FR Class I) radio sources is fundamentally different from the fueling of the strong emission-line AGN.

4. Black hole growth

4.1. Which black holes are growing?

Using the black hole masses derived for all bulge-dominated galaxies in the SDSS main galaxy sample, H04

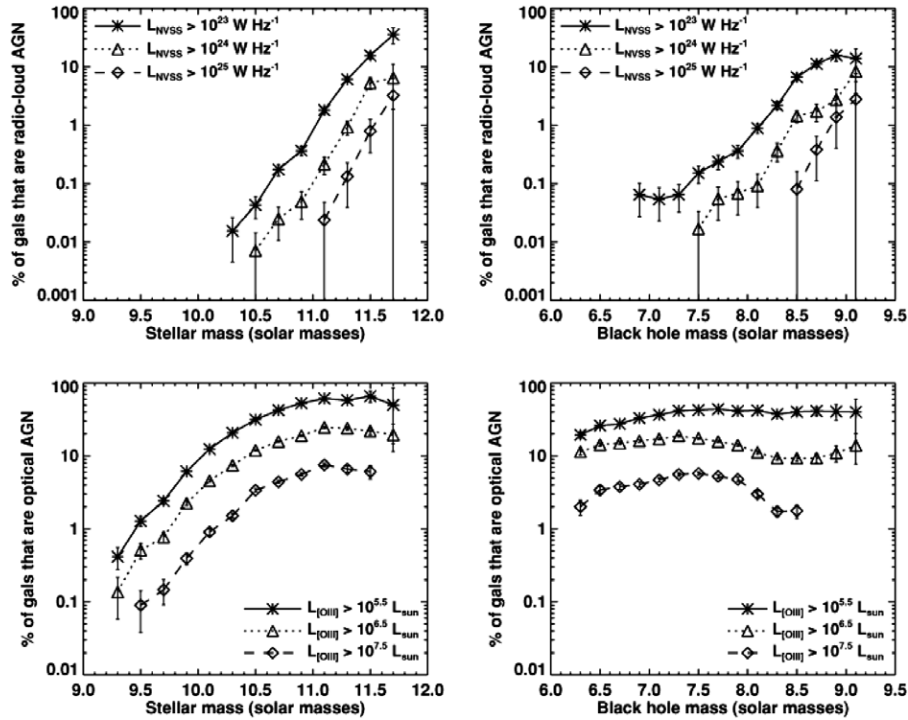


Fig. 2. Top: the fraction of galaxies that are radio-loud AGN, as a function of stellar mass (left) and black hole mass (right), for different cuts in radio luminosity. Bottom: the equivalent plots for optical emission-line selected AGN. See B05 for details.

showed how the total mass in black holes is partitioned among black holes of different masses. We found that the bulk of the mass resides in black holes with masses between $\sim 10^{7.5}$ and $10^{8.5} M_{\odot}$. However, using the AGN [OIII] emission-line luminosity to estimate mass accretion onto black holes, we found that the bulk of this accretion is occurring in black holes with significantly lower masses ($\sim 10^7$ to $\sim 10^8 M_{\odot}$) (see H04).

In Fig. 3, we take the ratio of the volume-integrated distributions of black hole mass and mass accretion rates as a function of black hole mass to compute the mass doubling time (growth time) for the present-day population of black holes as a function of black hole mass. This shows that the most rapidly growing population of black holes is that with $M_{\text{BH}} < \text{few} \times 10^7 M_{\odot}$, with an implied growth time of only a few tens of Gyr (twice the age of the universe). Above this mass, the growth time increases very rapidly to become orders of magnitude longer than the Hubble time. Alternatively, we can think of this in terms of a measure of the ratio of the current to the past-averaged growth rate of black holes. Our results indicate that for the population of low-mass black holes, this is around a half. In contrast, the population of more massive black holes ($> 10^8 M_{\odot}$) must have formed at significantly higher redshifts, as it is currently experiencing very little additional growth.

We have seen that the most massive black holes are associated with relatively low power radio sources. What about black hole growth associated with this phenomenon? For the radio-loud AGN we have used the results in Birzan et al. (2004) and the models by Bicknell (1995) to convert

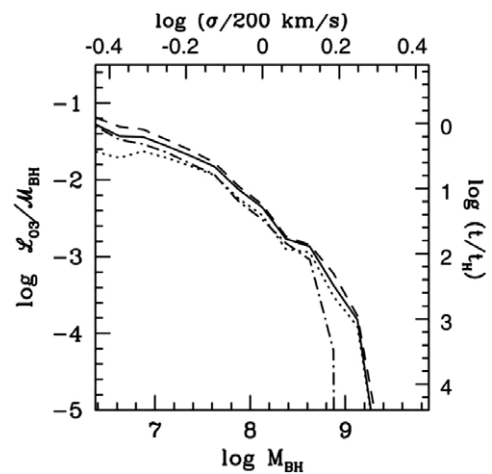


Fig. 3. The logarithm of the ratio of the total volume-weighted [OIII] luminosity in AGN to the total volume-weighted mass in black holes (both in solar units) is plotted as a function of velocity dispersion σ (upper axis) and $\log M_{\text{BH}}$ (lower axis). The right axis shows the corresponding growth time for the population of black holes in units of the Hubble time. See H04 for details.

the radio synchrotron luminosities into energy transport rates in the radio jets. For any plausible value for the ratio of black hole mass accretion rate to resulting energy outflow rate, we find that the rate of black hole growth associated with this mode is negligible (see B05). Apparently the most massive black holes (“dead QSOs”) only simmer today, with weak episodic **collimated** eruptions of relativistic plasma.

The basic result that black hole growth is “down-sizing” (moving to lower characteristic mass scales with cosmic time) is fully consistent with direct observations of the cosmic evolution of the AGN X-ray luminosity function (Ueda et al., 2003; Barger et al., 2005; Hasinger et al., 2005).

4.2. The co-evolution of black holes and bulges

We showed above that the population of low-mass black holes is still growing rapidly. If the tight relation between black hole mass and bulge mass is to be maintained in the “fossil record”, the host bulges of these systems must be “forming” at a comparable rate. In Fig. 4, we plot the ratio of the integrated star formation rate in *all* galaxies to the integrated accretion rate onto black holes, as traced by [OIII] emission from AGN. This is plotted as a function of black hole mass and of stellar surface mass density (see H04).

From this figure, it is clear that black hole growth is closely linked to star formation in the bulge. At low values of μ_* characteristic of disk-dominated galaxies, the ratio of SFR to black hole growth rises steeply. This is because very few of these galaxies host AGN, but there is plenty of star formation taking place in galaxy disks. At values of μ_* above $3 \times 10^8 M_\odot \text{ kpc}^{-2}$, the ratio remains roughly constant. Moreover, its value is ~ 1000 , which is in good agreement with the empirically-derived ratio of bulge mass to black hole mass (Marconi and Hunt, 2003). Note that the star formation rate estimated within the fiber is likely to underestimate the true star formation rate in the bulge, particularly for the largest and most massive galaxies. Conversely, the total SFR is probably an overestimate, because many galaxies will have star-forming disks. Given the uncertainties, we find it remarkable that the globally integrated ratio of star formation to black hole growth in the population of bulge-dominated galaxies comes out within

a factor of a few of the value that is expected from the $M_{\text{BH}}-M_{\text{bulge}}$ relation.

Finally, in Fig. 5 we compare the average growth time of the population of supermassive black holes with the average growth time of the population of galactic bulges in which they live. The growth time of the bulge is estimated from the ratio of the total stellar mass within the fiber aperture in these systems to the total star formation rate measured inside the fiber. We perform these integrals only over the bulge-dominated normal galaxy population. As can be seen, the black hole and bulge growth times track each other remarkably closely for galaxies with $M_* > 10^{10} M_\odot$. For low-mass bulges/black holes, the growth times are of the order of the Hubble time, but they increase by more than an order of magnitude for massive bulges/black holes. This is consistent with the fact that the smaller bulges in later type galaxies tend to be younger than the larger bulges in earlier type galaxies.

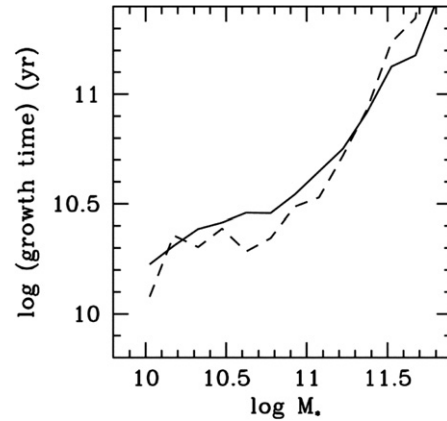


Fig. 5. The volume-averaged growth time of the galaxy population calculated within the SDSS fiber aperture (solid) is compared with that of the black hole population (dashed). Results have been plotted as a function of galaxy mass. Only AGN with $\log L_{\text{O3}} > 10^{6.5} L_\odot$ have been included in the estimation of black hole growth. See H04 for details.

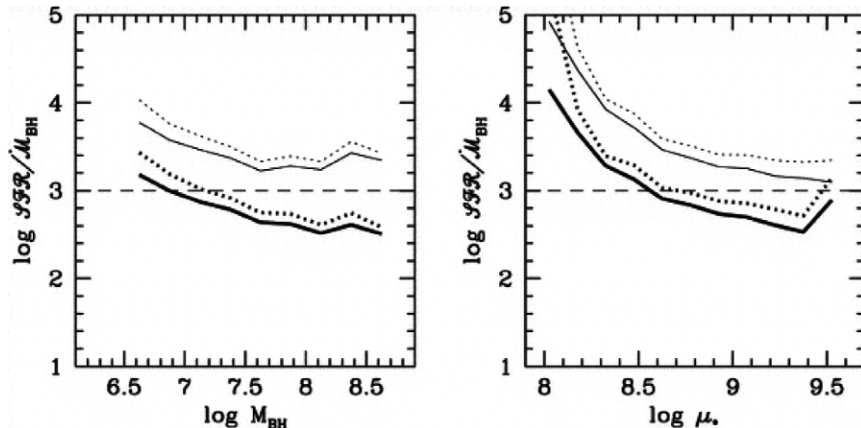


Fig. 4. The ratio of the total volume-weighted star formation rate in galaxies to the total volume-weighted accretion rate onto black holes as traced by AGN is plotted as a function of the black hole mass and the galaxy stellar surface mass density. The thick black lines show the result if SFR is calculated within the fiber aperture for each galaxy and the thin black lines show the result using estimates of total SFR. The dotted lines show results restricted to the AGN with $\log L_{\text{O3}} > 10^{6.5} L_\odot$. The dashed line shows the fiducial value of stellar to black hole mass in bulges and elliptical galaxies. See H04 for details.

5. Summary

We have used the analyses of two samples of AGN drawn from the main spectroscopic sample of galaxies in the Sloan Digital Sky Survey to summarize the relationship between AGN and galaxy properties in the present-day universe. One sample (see K03 and H04) consists of AGN identified on the basis of their narrow optical emission-lines. The other sample (B05) consists of AGN identified on the basis of their nonthermal radio emission. Both samples are large and complete, and have highly homogeneous data. We have used the SDSS spectra and images to measure or infer many of the fundamental properties of the galaxies (e.g. the mass, density, and mean age of the stellar population) and of the AGN (black hole mass, bolometric luminosity, mass accretion rate). Based on these analyses, we have reported the following conclusions:

- The SDSS galaxy population as-a-whole is strongly bimodal. One set (the bulge-dominated systems) are galaxies with high mass, high density, and high structural concentration. These have predominantly old stellar populations. The other (the disk-dominated galaxies) have low masses, low densities, and low concentrations. These have a substantial young stellar population. The transition between galaxies with young and old stellar populations is remarkably sharp at characteristic values for stellar mass, density, and concentration.
- The present-day growth of black holes (as traced by the emission-line AGN) is concentrated in galaxies lying near and just above the values of these structural parameters that delineate the boundary between the two galaxy populations.
- On-average, the more powerful emission-line AGN are hosted by galaxies with younger stellar populations. In particular, strong emission-line AGN are hosted by “hybrid” galaxies: they have the relatively high masses and densities of normal bulge-dominated galaxies, but a significant young stellar population like the disk-dominated galaxies. This is a relatively unusual combination in the SDSS galaxy population as-a-whole. In addition, there is evidence that an unusually large fraction of these galaxies have undergone a “starburst” in the past \sim Gyr.
- The relatively low-power (FR Class I) radio galaxies are the most massive galaxies, with structures and (old) stellar populations typical of giant elliptical galaxies. They are nearly orthogonal in their properties to the strong emission-line AGN.
- The present-day global ratio of star formation to black hole growth in the population of bulge-dominated galaxies has roughly the same ratio ($\sim 10^3$) as the ratio of stellar to black hole mass in individual bulges today.
- The population of low-mass black holes ($< 10^{7.5} M_{\odot}$) is growing today at a rate similar to the past-average. On the other hand, the population of the most massive black holes (“dead QSOs”) is experiencing negligible growth today (even accounting for any plausible amount of

accretion associated with powering the radio sources). These results imply that star formation and black hole growth have been moving steadily and in parallel to lower and lower mass scales due to a redshift of ~ 2 .

These results lead to a picture in which strong black hole growth is occurring only in those systems with the requisite combination of a substantial bulge and a supply of cold gas which fuels both star formation and the black hole. Could the cold gas be related to the accretion of gas-rich satellites (“minor mergers”) as galaxies continue to assemble hierarchically (e.g. Kauffmann et al., 2006)? A supply of cold gas is no longer available today in the most massive systems. In these objects, the recurrent low-level AGN activity may be fueled instead by the cooling of the hot X-ray gas (B05).

Acknowledgements

We would like to thank all our collaborators on the projects discussed in this paper. Special thanks to Philip Best who lead the effort on the analyses of the radio-loud AGN sample. Finally, we would like to thank the Sloan Digital Sky Survey collaboration for making it all possible.

Funding for the creation and distribution of the SDSS Archive has been provided by the Alfred P. Sloan Foundation, the Participating Institutions, the National Aeronautics and Space Administration, the National Science Foundation, the US Department of Energy, the Japanese Monbukagakusho, and the Max Planck Society. The SDSS web site is <http://www.sdss.org/>. The SDSS is managed by the Astrophysical Research Consortium (ARC) for the Participating Institutions. The Participating Institutions are The University of Chicago, Fermilab, the Institute for Advanced Study, the Japan Participation Group, The Johns Hopkins University, the Korean Scientist Group, Los Alamos National Laboratory, the Max-Planck-Institute for Astronomy (MPIA), the Max-Planck-Institute for Astrophysics (MPA), New Mexico State University, University of Pittsburgh, University of Portsmouth, Princeton University, the United States Naval Observatory, and the University of Washington.

References

- Baldwin, J., Phillips, M., Terlevich, R., 1981. *PASP* 93, 5.
- Barger, A., Cowie, L., Mushotzky, R., Yang, Y., Wang, W.-H., Steffen, A., Capak, P., 2005. *AJ* 129, 578.
- Becker, R., White, R., Helfand, D., 1995. *ApJ* 450, 559.
- Best, P., Kauffmann, G., Heckman, T., Brinchmann, J., Charlot, S., Ivezić, Z., White, S., 2005. *MNRAS* 362, 25.
- Bicknell, G., 1995. *ApJS* 101, 29.
- Birzan, L., Rafferty, D., McNamara, B., Wise, M., Nulsen, P., 2004. *ApJ* 607, 800.
- Blanton, M.R., Lupton, R.H., Maley, F.M., Young, N., Zehavi, I., Loveday, J., 2003. *AJ* 125, 2276.
- Boyle, B.J., Shanks, T., Croom, S.M., Smith, R.J., Miller, L., Heymans, N., Loaring, C., 2000. *MNRAS* 317, 1014.

- Brinchmann, J., Charlot, S., White, S.D.M., Tremonti, C., Kauffmann, G., Heckman, T.M., Brinkmann, J., 2004. *MNRAS* 351, 1151.
- Bruzual, G., Charlot, S., 2003. *MNRAS* 344, 1000.
- Condon, J. et al., 1998. *AJ* 115, 1693.
- Fan, X. et al., 2001. *AJ* 121, 31.
- Ferrarese, L., Merritt, D., 2000. *ApJ* 539, L9.
- Fukugita, M., Ichikawa, T., Gunn, J.E., Doi, M., Shimasaku, K., Schneider, D.P., 1996. *AJ* 111, 1748.
- Genzel, R., Pichon, C., Eckart, A., Gerhard, O.E., Ott, T., 2000. *MNRAS* 317, 348.
- Granato, G.L., Silva, L., Monaco, P., Panuzzo, P., Salucci, P., De Zotti, G., Danese, L., 2001. *MNRAS* 324, 757.
- Gunn, J., Carr, M., Rockosi, C., Sekiguchi, M., Berry, K., Elms, B., de Haas, E., Ivezić, Z., et al., 1998. *ApJ* 116, 3040.
- Hasinger, G., Miyaji, T., Schmidt, M., 2005. *A&A* 441, 417.
- Heckman, T., Kauffmann, G., Brinchmann, J., Charlot, S., Tremonti, C., White, S., 2004. *ApJ* 613, 109.
- Hogg, D., Finkbeiner, D., Schlegel, D., Gunn, J., 2001. *AJ* 122, 2129.
- Kauffmann, G. et al., 2003a. *MNRAS* 348, 333 (K03).
- Kauffmann, G. et al., 2003b. *MNRAS* 341, 33.
- Kauffmann, G. et al., 2003c. *MNRAS* 341, 54.
- Kauffmann, G., Haehnelt, M.G., 2000. *MNRAS* 311, 576.
- Kauffmann, G., Heckman, T., De Lucia, G., Brinchmann, J., Charlot, S., Tremonti, C., White, S., 2006. *MNRAS* 367, 1394.
- Marconi, A., Hunt, L.K., 2003. *ApJ* 589, L21.
- Marconi, A., Risaliti, G., Gilli, R., Hunt, L., Maiolino, R., Salvati, M., 2004. *MNRAS* 351, 169.
- Salpeter, E., 1964. *ApJ* 140, 796.
- Smith, J.A. et al., 2002. *AJ* 123, 2121.
- Stoughton, C. et al., 2002. *AJ* 123, 485.
- Strauss, M. et al., 2002. *AJ* 124, 1810.
- Tremaine, S. et al., 2002. *ApJ* 574, 740.
- Ueda, Y., Masayuki, A., Ohta, K., Miyaji, T., 2003. *ApJ* 598, 886.
- Veilleux, S., Osterbrock, D., 1987. *ApJS* 63, 295.
- York, D.G. et al., 2000. *AJ* 120, 1579.
- Yu, Q., Tremaine, S., 2002. *ApJ* 335, 965.
- Zakamska, N. et al., 2003. *AJ* 126, 2125.